ORIGINAL ARTICLE

Jean-Christophe Domec · Barbara L. Gartner

Cavitation and water storage capacity in bole xylem segments of mature and young Douglas-fir trees

Abstract Hydraulic specific conductivity, vulnerability to cavitation and water storage capacity of Douglas-fir sapwood was determined for samples from six young (1.0–1.5 m tall) and six mature trees (41–45 m tall). Measurements on samples from young trees showedthere were no effects of two contrasting sample types (entire stem segments vs sectors chiseled out of entire stems) on any of the calculated hydraulic parameters, for vulnerability to cavitation and water storage capacity. Measurements on mature trees were made on wood from four heights on the bole and from two sapwood depths. Outer and inner sapwood at the base of the tree had higher water storage capacities and were more vulnerable to cavitation than was sapwood from the tree top. At every height, old trees were more vulnerable to cavitation than at 1.0 m from the ground in young trees. The water storage capacities showed three distinct phases at the base of the trunk. Young trees had similar water storage capacity (per unit volume of sapwood) to the topof the mature trees, which was lower than the water storage capacity throughout the rest of the bole xylem. The way in which capacitance was calculated (on a volumetric basis vs a relative water content basis) affected the conclusion one would draw at the low water potentials (<–3 MPa). Within a tree, we found an apparent trade-off between having both hydraulic specific conductivity and stem water storage, and vulnerability to cavitation.

Keywords Douglas-fir [*Pseudostuga mensiesii* (Mirb.) Franco] · Cavitation · Embolism · Trunk vulnerability curve · Water storage capacity

J.C. Domec (✉) · B.L. Gartner
Department of Forest Products, Oregon State University,
Corvallis, Oregon, USA
e-mail: jc.domec@orst.edu
Tel.: +1-541-7374329, Fax: +1-541-7373385

Introduction

Methods now exist to quantify the effect of embolism on hydraulic conductivity (Sperry et al. 1987). These methods consist of measuring the flux of water perfused under moderate pressure difference (5 kPa) and steady-state conditions across an isolated stem segment that has been subjected to a given degree of water stress. This conductivity is then expressed as a percentage of the maximum conductivity obtained before water stress was imposed. By repeating this procedure with different samples at different pressure potentials, a vulnerability curve (VC) can be established. A VCexpresses the percentage loss of conductivity exhibited relative to the minimum water potential experienced by the sample.

The VCs published for woody plants in general and for Douglas-fir [*Pseudostuga mensiesii* (Mirb.) Franco] in particular have been for small seedlings or branches and roots (Cochard 1992; Sperry and Ikeba 1997; Kavanagh et al. 1999), but crucial information for the trunk is unknown. Current techniques to quantify vulnerability to embolism (e.g., Holbrook et al. 1995; Alder et al. 1997) are limited to small-diameter (<2-cm) round-wood (that necessitate the use of the entire xylem cross section), so absolutely no information on trunks or indeed any plants more than 2 cm in diameter has been assembled. Spicer and Gartner (1998a) developed a conductivity apparatus that allows determination of the hydraulic specific conductivity (k_s) of wood samples that are smaller than an entire stem cross section. This apparatus allows measurements of k_s of trunks, branches, and roots. This paper represents the first attempt to use this method in conjunction with the air-injection method to determine the VCs as well as the water storage capacity of mature tree trunks.

Within an individual, woody plants have a large range of anatomical and mechanical properties, varying within the bole both radially and vertically. Because of the differences in wood anatomy and density (Gartner 1995), it is logical to hypothesize that the top and the bottom of a tree would be characterized by wood of very different

hydraulic properties. We test the hypothesis that the top of the tree is less vulnerable to cavitation than the bottom because of smaller tracheid diameters (Panshin and De Zeeuw 1980), which are harder to embolize (Tyree et al. 1994), and that inner sapwood has lower resistance to cavitation than outer sapwood because it has "aged", or accumulated more damage to the conducting system. In addition, we tested whether the sample geometry affects VCs and values of water storage by comparing the air injection methods on entire cross sections of roundwood versus excised chunks from young trees. Finally it is surprising that among numerous studies on vulnerability to cavitation, there is still no simple method to analyze the VCs that can be compared between studies. We present coefficients that have a physiological significance, then use these coefficients to compare VCs between and within individual trees.

Materials and methods

Sample shapes test

Trunk segments were collected from six young (4-year-old) Douglas-fir trees from a nursery bed ranging from 1.0 to 1.5 m in height. Long stem segments were removed from the 3rd year of growth where the diameter under bark was small enough to fit entirely into a 1-cm-diameter double-ended pressure chamber. The whole segments were long enough to be divided into two smaller segments of 13 cm. The bottom segment was split into two parts along the grain with a chisel whereas the top segment was left intact, and the ends of all segments were recut with razor blades. Only one of the split segments was used from each tree.

The principle of the method was to measure the loss of conductivity on the prepared samples of trunk wood by alternately measuring conductivity in one apparatus and applying air pressure in a second apparatus. The first apparatus was a double-ended chamber (made of PVC) with a latex membrane that was pushed against the sample sides with a small positive pressure to keep fluid from leaving by the sample's sides rather than ends (Spicer and Gartner 1998a, b). The second apparatus was a double-ended pressure chamber that is used for the air-injection method (Salleo et al. 1992; Sperry and Saliendra 1994). We measured the initial hydraulic conductivity $k_{s(i)}$, then imposed a small positive air pressure (Ψ) on the sample to induce cavitation in the most vulnerable tracheids. Segments were then removed from the pressure chamber and submerged in water for about 15–35 min to permit diffusion of air bubbles into tracheids. The samples were freshly recut at each end after each pressurization, the hydraulic conductivity at

Ψ, $k_{s(\Psi)}$, was re-measured, and a larger pressure was then imposed. The pressure bomb was first pressurized to 0.5 MPa and stabilized with a valve regulator for 1 min, and then 1.0 MPa steps were used until more than 95% loss of $k_{s(i)}$ was reached. We established the VCs by graphing the proportion of saturated $k_{s(\Psi)}$ as a function of applied air pressure. We conducted several tests to assess whether there was a difference between the loss of conductivity for 1-min duration of pressurization and that for 10 min, but could detect none; this was consistent with the findings of Kavanagh et al. (1999) on branches and roots for the same species.

For the split segments, the conductivity apparatus as well as the method of measurement were taken from Spicer and Gartner (1998b). One end of the pressure sleeve was attached to tubing filled with filtered (0.22 μm) water adjusted with HCl to pH 2 in order to prevent microbial growth. The temperature of this solution was recorded before and after each hydraulic conductivity measurement. The distal end was attached to a 1-ml micropipette (0.01 ml graduation) and the flow through the segment was induced by a hydraulic head of pressure of 0.0052 MPa. We recorded the time for five consecutive intervals, observing the meniscus in the pipette as it passed successive tick marks. After measurements, sample lengths were measured (mm) then the cross-sectional area of each end was estimated by using the two tangential widths and one radial width. The solution was passed through 13-cm-long trunk sections ranging from 0.7 to 0.9 cm^2 in transverse area.

For the whole and intact segments, the differences in methodology were as follows: the conductivity measurements were made without surrounding the sample in the membrane-lined pressure sleeve, and transverse area was estimated with two perpendicular diameters.

Mature trunk measurements

Six Douglas-fir [*Pseudostuga mensiesii* (Mirb.) Franco] trees from the Cascade Range, Oregon, USA (42°57 N, 123°21 W) located at 220-m elevation were selected from the stand for experiments in late March 1998, before spring growth had started. The trees were selected to have no major forks or injury and to be of similar size and dominance. The trees averaged 43.7±1.3 m tall and were 100–120 years old. The morphological characteristics of the trees are shown in Table 1. Within hours of harvesting (on 27 March and 1 April), we cut four disks from each tree with an approximate thickness of 22 cm from the following internodes (counting from the top of the tree): 5, 15, 35, and from 1-m height above the ground (which represented 102–113 internodes, Fig. 1). These disks were transported in wet plastic bags, then stored at 5°C until blocks were prepared. From each disk, four blocks were cut within 3 days of felling the trees, two from the inner sapwood and two from the outer sapwood. Preparation of these specimens made from the blocks followed the procedures outlined by Spicer and Gartner (1998a, b). The specimens were split with a chisel along the grain, then stored in the dark at 5°C in water that was changed

Table 1 Mean values (± SE, *n*=6) for morphological characteristics of mature Douglas-fir trees by height position (node) counting down from the top of the tree, at 1 m from the ground, and at the base (about 30 cm). The base of the live crown was located a few nodes below node 35 at a mean height of 29±1 m. The whole sapwood width has been divided in two parts to determine the outer sapwood shell (comprised between the outer part of the sapwood and the middle of the sapwood width) and the inner sapwood shell (comprised between the middle of the sapwood width and the heartwood-sapwood boundary). The proportion of outer sapwood (%) has been calculated in dividing the outer sapwood shell by the total sapwood area

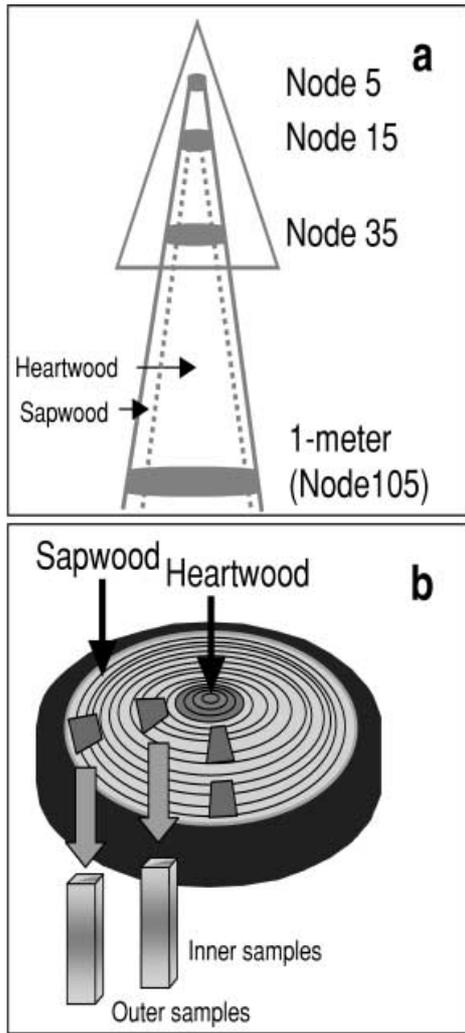| Height position	Mean height (m)	Diameter (cm)	Sapwood area (cm^2)	Heartwood area (cm^2)	Proportion of outer sapwood (%)	Number of sapwood rings
Node 5	42±2	3.5±0.5	7±1	0	100	4.8±0.2
Node 15	39±1	9.5±1.1	55±6	50±1	64±1	8.9±0.4
Node 35	35±1	20±1	222±2	61±12	60±1	15±1
1 m	1	64±2	760±10	1,766±117	52±1	29±2
Base	0.33±0.03	67±2	808±10	1,915±123	52±1	30±2

Fig. 1a, b Preparation technique for Douglas-fir samples. **a** Four disks were cut perpendicular to the trunk of the tree. One disk at node 5 counting down from the top of the tree, one at node 15, one at node 35 and one at 1-m height (corresponding to node 105). **b** For the first three disks, four samples were removed from two perpendicular sides in order to determine the hydraulic specific conductivity, the vulnerability to cavitation, and the water storage capacity. Two samples were taken in the inner part of the sapwood (two rings before the sapwood-heartwood transition), and two other samples in the outer part (youngest rings formed). Forthe upper disk (node 5), only two samples were taken in the outer part. The disk represented as an example is from node 15

daily, until they were used within 3 weeks of preparation. After each measurement the number of days (ranging from 1 to 21) was computed to determine the effect of time storage. Determination of the VCs for each segment from the six trees followed the same method as that described above for the young trees. The storage time was unavoidable because trees had to be harvested in one trip, and then after preparation it required about 6 h to produce a VC on each sample.

Calculation of specific conductivity

Sapwood specific conductivity was calculated according to Darcy's law (Edwards and Jarvis 1982):

$$k_s = \frac{V \cdot L \cdot \eta}{t \cdot A \cdot \Delta P} \qquad (1)$$
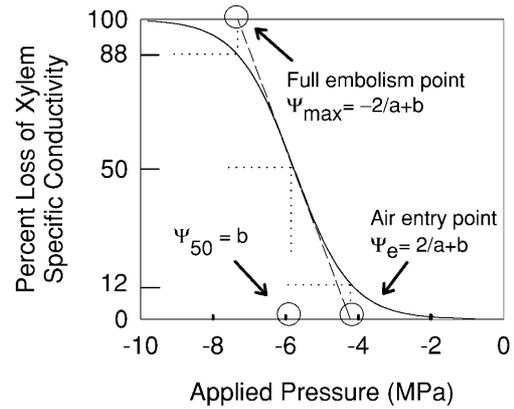

Fig. 2 Method of determining xylem air-entry point (Ψ_e) and full embolism point (Ψ_{max}) based on vulnerability curves data. The vulnerability curves are calculated using both parameters a and b (Eq. 3). The percent loss of hydraulic conductivity plotted versus the pressure applied results in a linear phase where the cavitation jump occurs. The air entry point and the full embolism point represent 12% and 88% loss of xylem hydraulic conductivity respectively (Eqs. 5, 6). The slope of the *dashed line* tangential to the point ($\Psi_{50}=b$, 50) is equal to $a.100/4$ (Eq. 7)

where V is the volume of water that went through the sample (m^3), L is the sample length (m), η is the viscosity of water at the temperature at which the experiments were conducted (N s m^{-2}), t is the time (s), A the cross-sectional area (m^2) of the sample and ΔP is the pressure difference (Pa) between ends of the sample. The entire cross section of each sample was assumed to be functional sapwood and was calculated from the average of the cross-sectional areas of the two ends.

Calculation of coefficients from VCs

The percentage loss of conductivity at a given pressure was calculated using the following equation (Sperry and Tyree 1988):

$$\% loss\_k_{s(\psi)} = \frac{(k_{s(i)} - k_{s(\psi)})100}{k_{s(i)}} \qquad (2)$$

In this equation $k_{s(i)}$ is the initial specific conductivity and $k_{s(\psi)}$ is the conductivity measured after air had been injected at a positive pressure, Ψ. A plot of these datais called a vulnerability curve. The relationship between loss of conductivity and the applied pressure can be described by the following sigmoidal equation (e.g., Pammenter and Vander Willigen 1998):

$$\% loss\_k_{s(\psi)} = \frac{100}{(1 + e^{a(\psi-b)})} \qquad (3)$$

The coefficient a is an indicator of the slope and the coefficient b represents the tension at which 50% loss of conductivity occurred (denoted as $b=\Psi_{50}$).

We analyzed these data further by looking at the values from the derivative of Eq. 3. In this manner, more information could be gleaned and compared between different VCs. The derivative of Eq. 3 is:

$$\frac{d(\% loss\_k_{s(\psi)})}{d\psi} = \frac{-a(e^{a(\psi-b)})100}{(1 + e^{a(\psi-b)})^2} \qquad (4)$$

The derivative gives us the slope of each tangential line at an applied pressure, Ψ. If one calculates the derivative for the point on the curve where the loss of k_s is 50% (% loss $k_{s(b)}$=50%), one can then calculate the intercepts of the derivative at % loss $k_{s(\psi)}$=0% as (Fig. 2):

$$\Psi_e = 2/a + b \qquad (5)$$

and %loss_$k_{s(\Psi)}$ = 100% as:

$$\Psi_{max} = -2/a + b \tag{6}$$

The value Ψ_e is termed the air-entry point (Sparks and Black 1999) and is an estimate of the xylem tension at which pit membranes are overcome within the conducting xylem and when cavitation starts. It is only a linear approximation of the true air entry point, which may start very close to $\Psi=0$ (as in Fig. 2), but it is a very useful way to compare different curves. Likewise, we termed Ψ_{max} the full embolism point and it is interpreted as approximating the actual maximum tension of the xylem before failing and becoming non-conductive. The applied pressures at air entry point and at full embolism point represent respectively 11.92% and 88.08% loss of xylem hydraulic conductivity.

Finally, one can also derive the actual slope (s) of the linear part of the VC from Eq. 4 (Fig. 2) as:

$$s = a \cdot 100/4 \tag{7}$$

where s is in % loss k_s MPa^{-1} and can be used as an estimate of the slope of the conductivity loss versus xylem water potential. As suggested by Sperry (1995), the steeper the slope, the more conservative the evolved strategy of the xylem due to a smaller safety margin between Ψ_e and Ψ_{max}.

Water storage capacity

For each conductivity measurement, the mass and the volume of the specimens were measured. Mass was determined on a balance after samples were dried using paper towel, and volume was determined from mass displacement of the specimen in a beaker of water on a balance (Borghetti et al. 1991). After the last cycle, the specimens were reweighed after drying at 104°C. Relative water content (RWC) was calculated as follows:

$$RWC = \frac{M_f - M_d}{(V_f - V_s) D_{H2O}} \tag{8}$$

where D_{H2O} is the density of water (g cm^{-3}); M_f and M_d are the fresh and dry mass of the wood (g), respectively; V_f is the fresh volume of the sample (cm^3); and V_s is the volume of solid material (cm^3) (pure cell wall material, without air or water). The volume of solid material was calculated from the dry mass assuming that dry cell-wall material has a density of 1.53 g cm^{-3} (Siau 1984).

Water storage capacity can be defined as the amount of water withdrawn from the stem at a given water potential (Holbrook 1995). Most of the time and for comparative reasons, capacitance is expressed as the change in water mass relative to the sample volume per unit change in water potential. The volumetric capacitance (C_V) between 0 and 5.0 MPa was determined after each conductivity test as follows (Running 1980; Edwards and Jarvis 1982; Tyree et al. 1991):

$$C_V = \frac{d\left(\dfrac{(M_f - M_d)}{V_f}\right)}{d\psi} \text{ in kg l}^{-1} \text{ MPa}^{-1} \tag{9}$$

Because wood is a porous material of variable density, we also expressed the capacitance as the change in RWC per unit change in water potential. This latter expression allows us to compare differences in storage capacities for samples differing both in total water volume and wood density. The RWC-based capacitance (C_{RWC}) between 0 and 5.0 MPa can be defined as:

$$C_{RWC} = \frac{dRWC}{d\psi} \text{ in RWC MPa}^{-1} \tag{10}$$

For the mature trunk measurements, to determine whether the slope of the dehydration curve was constant throughout its range, we also computed capacitancevalues for three phases in each dehydration curve (Tyree and Yang 1990): a phase from 0 to 0.5 MPa ($C_{0-0.5}$), a phase from 0.5 to 3.0 MPa ($C_{0.5-3}$) and a phase from 3.0 to 5.0 MPa (C_{3-5}). According to Tyree and Yang (1990), these three phases dealt with water released by capillaries, water released by both capillaries and cavitation events, and water released by cavitation events only.

Statistical analysis

For the sample shapes test, paired t-tests were used to test differences in hydraulic parameters, a, b, Ψ_e, Ψ_{max}, and the slopes of the dehydration curves, between split and whole seedling trunks.

For the mature tree trunks, the VCs were fitted by the least square methods on the empirical model described in Eq. 3 conducted with Sigma Plot 5.0 for Windows (1999, Jandel Scientific Software, San Rafael, Calif.). Each sample was used as a single replicate that gave a single value of each a and b. The values of a, b, Ψ_e, and Ψ_{max} were compared among locations (two radial and four height positions) by carrying out an analysis of variance (ANOVA) and covariance (ANCOVA) using a strip-plot randomized complete block design (trees as block) with radial position and height position being the strip plots factors. In the strip plot design, which is a modification of the split plot design, observations are made on sets of "wholeunits". Unlike the split plots design, there are no split plots within whole (main) plots. Rather, the subunit treatments are applied in strips across an entire replication of main plot treatments. This arrangement facilitates mathematical manipulations concerning the subunits (these are easier to apply) but sacrifices precision in comparing the main effect of a treatment (SAS 1996). We used ANCOVA specifically to test for the significance of a covariate, the number of days of running the sample after preparation and initial RWC, while controlling for the effect of k_s.

The values of capacitance for a given range of pressures were compared among position with ANOVA using a strip-plot randomized complete block design (trees as block) with radial position and height position as the strip plots factors and with repeated measures in the procedure (repeated measures being the three different capacitances because they are inter-dependent and correlated over the range of applied pressures). The experiment was designed to assess values at both inner and outer sapwood, but for height position, we were interested in an estimate of the entire sapwood. Therefore, the effect of height position on the vulnerability parameters and on both measures of capacitances (C_v and C_{rwc}) was made by weighting the values by the proportion of the total sapwood area occupied by the outer and inner sapwood shells (Table 1). The inner shell represented the area from the third growth ring exterior to the heartwood/sapwood boundary to the middle of the sapwood zone, and the outer shell represented the area from the middle of the sapwood zone to the cambium.

Least square (LS) means were generated from a PROC MIXED procedure, and multiple comparisons among means were calculated using least square differences (LSD). All statistical procedures were conducted with Statistical Analysis Systems software (1996; SAS, Cary, N.C.).

Results

Sample shapes test

Whole stems and pieces of stems taken from Douglas-fir seedlings had similar VCs (Fig. 3), with respective values s (slope of the linear part of the VCs) of 28.0% and 29.8% loss k_s MPa^{-1}. Neither the vulnerability parameters, nor the estimated capacitances differed between the whole and split stems ($P>0.31$, paired t-test, data not shown). The values of Ψ_e (the air-entry point) for the whole and split stems were −3.4 and −3.2 MPa respectively. The values of Ψ_{max} (the full embolism point) for the whole and split stems were −7.9 and −8.0 MPa, respectively.
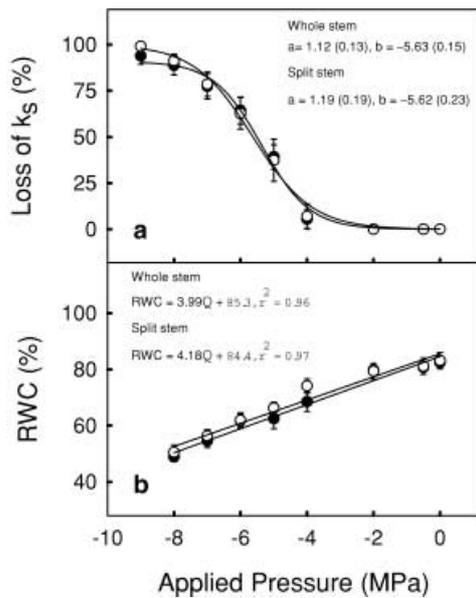
Fig. 3 Relationship between **a** vulnerability curves and **b** relative water content (*RWC*) for Douglas-fir seedlings showing the percentage loss of xylem hydraulic conductivityversus the negative of air pressure used in air injection experiments (*n*=6 for each injection mean; *error bars* are standard errors, vulnerability parameters from Eq. 3 and stem capacitances are shown in the figure with the SE in parentheses). *Filled symbols* are for the split stem and *open symbols* are for the whole stem
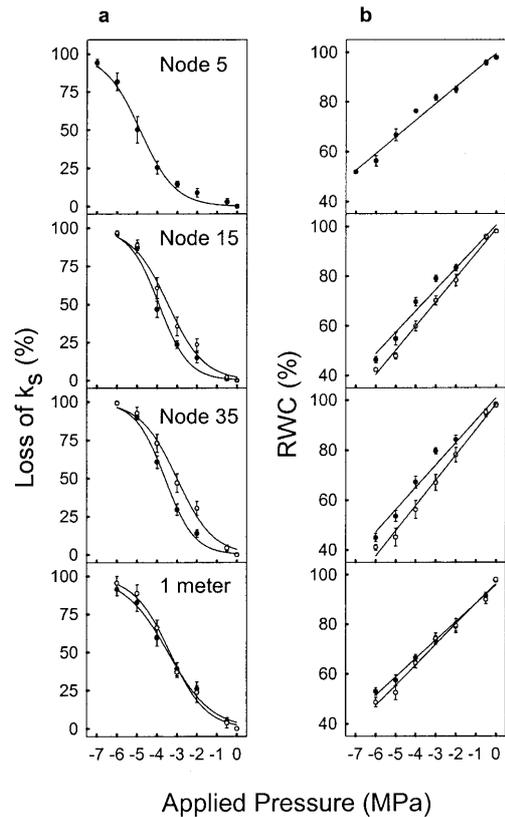

Fig. 4 a Loss in conductivity and **b** relative water content (*RWC*) versus applied air pressure in six mature Douglas-fir trees at four heights in the trunk (node 5, node 15, node 35 from the top and 1 m from the base) and two radial positions (outer and inner sapwood). Within the tree, the base had a higher water storage capacity than the top (see first column, Table 4 for the linear regression coefficients and statistical comparisons among height and radial positions) and was more vulnerable to cavitation than the top. *Error bars* are standard errors. *Filled symbols* are for the outer sapwood and *open symbols* are for the inner sapwood

The mean C_V (capacitance on a volumetric basis) was 0.037 and 0.036 kg l^{-1} MPa^{-1} for whole and split stems respectively. The minimum capacitances were between 0.5 and 2.0 MPa. The minimum C_V was 0.021 and 0.017 kg l^{-1} MPa^{-1} for the whole and split stems respectively. The minimum C_{RWC} (capacitance on the basis of relative water content) was 1 and 2% RWC MPa^{-1} for the whole and split stems, respectively.

Trunk vulnerability to cavitation

For both measures of RWC and percent loss of conductivity, blocking on trees was effective: the estimate of variation between trees was more than zero. This difference means that the variation of our experimental units (height and radial positions) was greater between the trees than within the trees. By accounting for these intrinsic differences among our experimental units, we obtained a smaller experimental error and improved the precision with which we estimated the effects of height and radial positions (Newman et al. 1997). K_s was neither related to the number of days after preparation nor the RWC of the sample (*P*>0.05, ANCOVA).

The tips of old trees were more vulnerable to cavitation than the tips of young trees (compare Fig. 3a and top panel, Fig. 4a). Additionally, for the outer sapwood, the top of the tree (node 5) had a significantly higher resistance to cavitation than node 35 and 1 m for all three parameters Ψ_e, Ψ_{50} (the tension at which 50% of conductivity is lost) and Ψ_{max} and than node 15 for the two parameters Ψ_{50} and Ψ_{max} (Table 2). For the inner sapwood, there was no significant difference between the base, node 35, and node 15 for any of the parameters calculated from the VCs. There was, however, a marginally significant interaction between disk position and the sapwood radial position for the first three heights for both Ψ_e ($F_{2,10}$=4.14, *P*=0.0491) and Ψ_{50} ($F_{2,10}$=4.12, *P*=0.0497).

In an ANOVA with height and radial position as fixed effects for the lower three heights, there was no significant difference between the overall inner and outer sapwood for either Ψ_e ($F_{1,5}$=6.47, *P*=0.052) or Ψ_{max} ($F_{1,5}$=2.77, *P*=0.16). There was a significant difference for Ψ_{50} between the overall inner and outer sapwood ($F_{1,5}$=6.98, *P*=0.041). This effect resulted from the significant difference between the outer and inner samples at node 35. Indeed, by position inner sapwood was only significantly less resistant to cavitation (*P*<0.0045) than outer sapwood at node 35 (approximately base of the live crown) where Ψ_e and Ψ_{50} are respectively 0.9 MPa

Table 2 Effect of height and radial position in the tree on the slope of the linear portion of the vulnerability curve (*s*), the potential (*b*) at which 50% loss of k_s is reached, the air entry point (Ψ_e) and the full embolism point (Ψ_{max}). The loss of xylem conductivity at Ψ_e and Ψ_{max} are 12% and 88% respectively. The initial rela- tive water content (*RWC*) of the samples is also given. Values with different letters within a column are significantly different (*P*<0.05). LS means (±SE, *n*=6) were generated from the PROC MIXED procedure, and multiple comparisons among means were calculated using LSD

Radial position	Height position	$s=a.100/4$ (%loss k_s MPa^{-1})	Ψ_e (MPa)	$b=\Psi_{50}$ (MPa)	Ψ_{max} (MPa)	RWC (%)
Outer sapwood	Node 5	30.4±4.7 ab	−3.1±0.3 a	−4.7±0.2 a	−6.4±0.3 a	97.8±0.4 a
	Node 15	40.2±4.4 a	−2.3±0.3 ab	−3.7±0.2 b	−5.1±0.3 bc	97.9±0.4 a
	Node 35	37.1±4.4 ab	−2.1±0.3 b	−3.5±0.2 b	−4.9±0.3 bc	98.1±0.4 a
	1 m	27.0±4.4 b	−1.3±0.3 c	−3.3±0.2 bc	−5.4±0.3 b	97.6±0.4 a
Inner sapwood	Node 15	32.5±4.4 ab	−1.7±0.3 bc	−3.4±0.2 bc	−5.0±0.3 bc	97.9±0.4 a
	Node 35	35.0±4.4 ab	−1.2±0.3 c	−2.9±0.2 c	−4.6±0.3 c	97.8±0.4 a
	1 m	30.3±4.5 ab	−1.5±0.3 c	−3.3±0.2 bc	−5.1±0.3 bc	97.8±0.4 a

Table 3 Effect of height position in the tree on the slope of the linear portion of the vulnerability curve (*s*), the potential (*b*) at which 50% loss of k_s is reached, the air entry point (Ψ_e) and the full embolism point (Ψ_{max}). The loss of xylem conductivity at Ψ_e and Ψ_{max} are 12% and 88% respectively. Values with different letters within a column are significantly different (*P*<0.05). LS means (±SE, *n*=6) were generated from the PROC MIXED procedure, and multiple comparisons among means were calculated using LSD

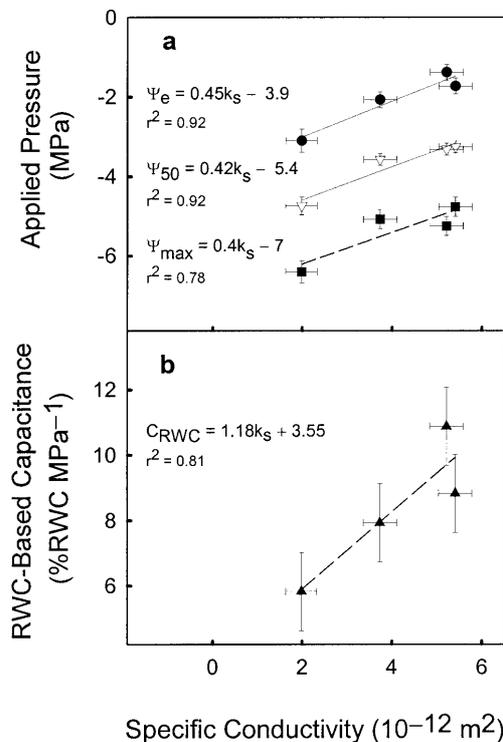| Height position	$s=a.100/4$ (%loss k_s MPa^{-1})	Ψ_e (MPa)	$b=\Psi_{50}$ (MPa)	Ψ_{max} (MPa)
Node 5	30.4±4.4 a	−3.1±0.3 a	−4.7±0.2 a	−6.4±0.3 a
Node 15	33.7±3.9 a	−2.1±0.2 b	−3.6±0.2 b	−5.1±0.2 c
Node 35	33.0±3.9 a	−1.8±0.2 b	−3.3±0.2 b	−4.8±0.2 b
1 m	25.9±3.9 a	−1.4±0.2 c	−3.3±0.2 b	−5.2±0.2 c

Fig. 5 a Trunk xylem hydraulic safety versus trunk xylem hydraulic efficiency of Douglas-fir trees. Xylem safety is represented by mean air entry tension (Ψ_e *filled circles*), mean cavitation tension (Ψ_{50}, *open triangles*) and maximum cavitation tension (Ψ_{max}, *filled squares*). Xylem efficiency is represented by the mean specific conductivity. **b** RWC-based capacitance versus mean specific conductivity. Xylem water storage capacity is represented by the mean RWC-based capacitance from 0 to 5 MPa (*filled triangles*). *Error bars* are standard errors
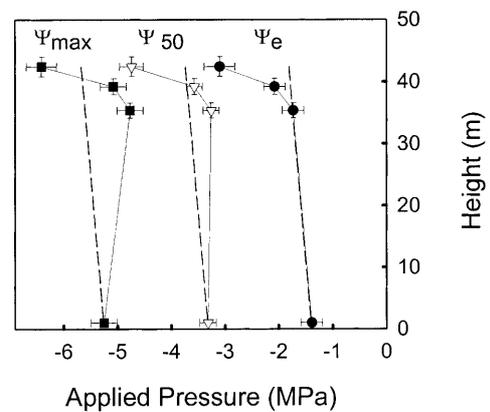

Fig. 6 Hydraulic safety of trunk xylem versus height in mature Douglas-fir. Xylem safety is represented by mean air entry tension (Ψ_e, *filled circles*), mean cavitation tension (Ψ_{50}, *open triangles*) and maximum cavitation tension (Ψ_{max}, *filled squares*). The theoretical hydrostatic gradient (0.01 MPa m^{-1}) has been plotted for each parameter based on their 1-m value (*dotted lines*). *Error bars* are standard errors

and 0.6 MPa higher than the outer sapwood measurements (Fig. 4a, Table 2). This pattern is not observed at the base of the tree (*P*>0.75) or at node 15 (*P*>0.075).

For the lower three disks, there was no evidence (Table 3) of a position effect for either Ψ_e ($F_{2,10}$=2.11, *P*=0.17) or Ψ_{50} ($F_{2,10}$=1.29, *P*=0.32). However, if we include the top of the tree (node 5), the difference between positions becomes highly significant for both parameters Ψ_e ($F_{3,14}$=13.06, *P*=0.0002) and Ψ_{50} ($F_{3,14}$=10.10, *P*=0.0023). There was no evidence of a position effect

Table 4 The first two columns represent the effect of radial and height position in the tree on the linear regression coefficients, slope (%RWC MPa⁻¹) and intercept (%RWC), of the relationship between RWC (%) and applied pressure (MPa). The slopes ($r^2 > 0.97$, $P < 0.01$) represent the average capacitance over the total range of pressure applied. The next three columns represent the effect of radial and height positions in the tree on the RWC-based capacitances (%RWC MPa⁻¹) for the three phases $C_{0-0.5}$ (between 0 and 0.5 MPa), $C_{0.5-3}$ (between 0.5 and 3.0 MPa), and C_{3-5} (between 3.0 and 5.0 MPa). Values with different letters within a column are significantly different ($P < 0.05$). LS means ($\pm$SE, $n=6$) were generated from the PROC MIXED procedure, and multiple comparisons among means were calculated using LSD

| Radial position | Height position | Regression parameters | | $C_{0-0.5}$ | $C_{0.5-3}$ | C_{3-5} |
		Slope	Intercept			
Outer sapwood	Node 5	6.7±0.4 b	99.4±1.4	4.7±1.9 a	5.0±0.8 a	7.8±1.3 a
	Node 15	8.6±0.6 ac	100.5±2.1	4.6±1.9 a	6.1±0.7 a	12.2±1.2 b
	Node 35	8.9±0.6 ac	100.6±2.3	7.6±1.8 a	5.7±0.7 a	11.6±1.2 b
	1 m	7.4±0.3 b	95.9±1.0	12.6±1.8 b	6.7±0.7 a	13.1±1.1 b
Inner sapwood	Node 15	8.8±0.3 ac	98.9±1.1	5.0±1.9 a	9.3±0.7 b	11.2±1.2 b
	Node 35	10.1±0.4a	98.3±1.5	5.0±1.8 a	11.2±0.7 c	10.6±1.2 b
	1 m	8.2±0.4 ac	96.4±1.5	15.9±1.8 b	6.2±0.7 a	10.9±1.2 b

on s for the four disks ($F_{3,14} = 2.23$, $P = 0.15$). Node 5 was significantly different than the other three heights ($P < 0.05$) for any of three parameters calculated. Between the other positions, the parameter Ψ_e at node 15 and 35 was significant lower than at the base of the tree ($P = 0.04$).

Using the data from the four disks in the tree, we asked whether there was a relationship between k_s and Ψ_e, Ψ_{50}, and Ψ_{max} (Fig. 5a). The slopes of straight lines were significantly different from zero at the 5% confidence level and were not statistically different from one another ($P = 0.76$, ANOVA). There was a significant positive correlation for both Ψ_e and Ψ_{50} but not for Ψ_{max}.

Using the data from the four disks in the tree, we asked whether there was a relationship between sampling height and calculated parameters of the VCs (Ψ_e, Ψ_{50}, and Ψ_{max}, Fig. 6). For Ψ_e, the slope of the portion of the line between the first two heights (the unbranched parts of the trunk between 1 m and node 35) was –0.0101 MPa m⁻¹ and was parallel to the theoretical hydrostatic gradient shown by the dotted line (–0.0100 MPa m⁻¹). This slope was zero for Ψ_{50} and positive for Ψ_{max} (0.0141 MPa m⁻¹). Within the crown (from nodes 35 to 5), the relationship between VC parameters and the heights had steeper slopes (–0.19, –0.21 and –0.23 MPa m⁻¹ respectively for Ψ_e, Ψ_{50}, and Ψ_{max}).

Trunk water storage capacity

RWC showed a linear change with applied pressure, with significantly steeper slopes from the top to the bottom of the tree ($P < 0.05$, Fig. 4b, Table 4). The overall trunk water capacitance was higher for the unbranched (below node 35) than for the branched part of the trees (Table 5). The top of the mature trees had similar water storage capacity to the young trees. Note that capacitance as discussed here is on a tissue volume basis, not to be confused with water storage capacity, which takes into account the capacitance and the quantity of a tissue.

Table 5 Effect of height position in the tree on the RWC-based capacitances (%RWC MPa⁻¹) for the three phases $C_{0-0.5}$ (between 0 and 0.5 MPa), $C_{0.5-3}$ (between 0.5 and 3.0 MPa), and C_{3-5} (between 3.0 and 5.0 MPa). Values with different letters within a column or/and a row are significantly different ($P < 0.05$). LS means ($\pm$SE, $n=6$) were generated from the PROC MIXED procedure, and multiple comparisons among means were calculated using LSD

Height position	$C_{0-0.5}$	$C_{0.5-3}$	C_{3-5}
Node 5	4.7±1.7 a	5.0±1.5 a	7.8±1.2 a
Node 15	4.7±1.7 a	7.3±1.4 a	11.8±1.4 b
Node 35	7.3±1.6 a	8.0±1.4 a	11.2±1.4 b
1 m	14.1±1.6 b	6.5±1.4 a	12.1±1.4 b

Even though there was a strong linear relationship between the RWC and the applied pressure for the whole ranges of pressure (Table 4), we separated the dehydration curves into three different phases ($C_{0-0.5}$, $C_{0.5-3}$, and C_{3-5}, Tables 4, 5, 6) corresponding to the three phases described by Tyree and Yang (1990). At the base of the tree, there was no significant difference in outer and inner sapwood for a given phase (Table 4). In an ANOVA with height and radial position as fixed effects, there was no significant difference between the overall inner and outer sapwood for either $C_{0-0.5}$ ($F_{1,5} = 0.56$, $P = 0.60$) or C_{3-5} ($F_{1,5} = -2.01$, $P = 0.10$). There was, however, a significant difference in $C_{0.5-3}$ between the overall inner and outer sapwood ($F_{1,5} = 5.07$, $P = 0.039$). For the first three disks, this effect is due to the significant difference between the outer and inner samples at node 35 and 15 (Table 4).

For the four disks in the tree, we asked whether there was a global relationship between $C_{0-0.5}$, $C_{0.5-3}$, and C_{3-5}. There was a significant difference in water storage capacity between $C_{0-0.5}$ and C_{3-5} ($F_{2,74} = -3.59$, $P = 0.006$) and between $C_{0.5-3}$ and C_{3-5} ($F_{2,74} = -4.82$, $P < 0.001$). Dehydration isotherms did not showsignificant differences between the three phases for the top of the tree only ($F_{2,74} < -1.69$, $P > 0.09$, Tables 5, 6). The mean water

Table 6 Effect of height position in the tree on the volumetric capacitances (kg l^{-1} MPa^{-1}) for the three phases $C_{0-0.5}$ (between 0 and 0.5 MPa), $C_{0.5-3}$ (between 0.5 and 3.0 MPa), and C_{3-5} (between 3.0 and 5.0 MPa). Values with different letters within a column or/and a row are significantly different ($P<0.05$). LS means ($\pm$SE, $n=6$) were generated from the PROC MIXED procedure, and multiple comparisons among means were calculated using LSD. To convert these values to dry weight basis (kg MPa^{-1} kg^{-1}) multiply the table values by 0.46, 0.42, 0.41 and 0.51 kg l^{-1} respectively for node 5, node 15, node 35 and 1 m. This change does not change the significance values except for C_{3-5} at 1 m that becomes significantly different than C_{3-5} at node 5, and for $C_{0-0.5}$ at node 15 that becomes significantly different than $C_{0.5-3}$ and C_{3-5} at node 15

Height position	$C_{0-0.5}$	$C_{0.5-3}$	C_{3-5}
Node 5	0.035±0.012 a	0.036±0.012 a	0.055±0.012 a
Node 15	0.035±0.012 a	0.053±0.011 a	0.086±0.011 b
Node 35	0.051±0.011 a	0.057±0.011 a	0.090±0.011 b
1 m	0.096±0.011 b	0.046±0.011 a	0.065±0.011 a

storage capacity did not change for the tip of the trunk. For $C_{0.5-3}$, and for both definitions for water storage capacity, we did not find any significant difference between the different locations in the trunk ($F_{2,74}<0.64$, $P>0.52$). On a RWC basis, the $C_{0-0.5}$ was significantly higher for the bottom of the tree and C_{3-5} lower for the tip than for the other locations (Table 5). For the volume basis the C_{3-5} for the top of the tree behaved like the bottom ($F_{2,74}=0.62$, $P=0.54$, Table 6).

The overall RWC-based capacitance increased sharply with an increase in k_s (Fig. 5b), from approximately 5% RWC MPA^{-1} at node 5 to 10% RWC MPa^{-1} at the base. Using the total height and sapwood area at each position in the tree (Table 2), we estimated a total water storage capacity between 0.5–3.0 MPa of 59 l per unit change in water potential (that represents 7% of the total volume of water of the sapwood) and 78% of this total water storage capacity comes from the trunk below node 35, which itself averaged several nodes below the average base of the crown.

Discussion

Methodological issues

Using the material from young trees, we found statistically inseparable results for samples prepared using the split segments and those prepared using roundwood for parameters of the vulnerability curves (Fig. 3). This finding shows that damage to sample edges has no significant effect on sample conductivity or vulnerability to cavitation, validating the appropriateness of this technique for this type of study and plant material. The open edges of the samples did not affect the responses of the loss of hydraulic conductivity to an applied pressure. The hypothesis that too many openings in the sample could create more cavitation and underestimate the RWC is therefore not valid for trunk and roundwood of this

species, so air-injection techniques can be used to measure the vulnerability to cavitation on raw pieces of wood subsampled from xylem segments of very large size, and not only from excised branches.

There was no measured effect of storage duration on conductivity, capacitance, or vulnerability parameters. This result suggests that changing the water every day and storing samples in the dark are efficient in the preventing value-altering microbial growth. When western hemlock (*Thuja occidentalis* L.) wood samples were stored at room temperature, their specific conductivity decreased by 34% after 2 weeks (Lin et al. 1973). When our samples were stored at 5°C in clean water, their specific conductivity did not decrease statistically even after 21 days. This result agrees with Erickson's study (1960) of permeability of Douglas-fir and western hemlock sapwood. He showed that storage in water at 5°C started to produce a lower rate of k_s after 1 month, with markedly lower rates if stored in bags without water.

The way in which capacitance was calculated affected the conclusion one would draw at the low water potentials (Tables 5, 6). The difference between the two methods of expression is of importance because of the changes in wood density by height and radial position. The use of the volumetric capacitances is confounded bytrends of variation in the wood density, and can be used only to compare specimens with the same density. For example if a sample with low density wood (top of the tree) is compared with a denser one (bottom of the tree), the specimens may have the same volumetric capacitances but the denser wood will contain less water and in fact will have a higher storage capacity based on its total available water present in the lumen cells. This trend is more obvious for more negative water potentials because the amount of water present is already far from saturation.

The capacitances we found from 0–0.5 MPa xylem tension are lower than those estimated for the same species by Waring and Running (1978, Fig. 2) (130% RWC MPa^{-1} and 0.65 kg l^{-1} MPa^{-1}) and for Scots pine (*Pinus sylvestris* L.) by Waring et al. (1979, Fig. 1) (110% RWC MPa^{-1} and 0.50 kg l^{-1} MPa^{-1}), but are similar for higher values of water potential (6% RWC MPa^{-1} and 0.30 kg l^{-1} MPa^{-1}). They reported that samples lost around 60% of their water between xylem tensions of 0 and 0.5 MPa. First, the discrepancy in capacitances at high water potential can be explained by the fact that Waring and Running (1978) and Waring et al. (1979) used wood samples that were cut into small flat disks (18 mm diameter by 4 mm in the tree's axial direction). Their proportion of cut-open tracheids was too high to estimate capacitances correctly because the water inside a cut-open tracheid is only held by capillarity, rather than capillarity and the tension within the xylem stream (Tyree and Yang 1990) so those studies overestimated capacitance in this range of water potentials. Secondly, our estimates in the range of water potentials from 0 to 0.5 MPa were also inaccurate, underestimating the water held by capillarity

but accurately estimating the water released by cavitations. Unlike Waring and Running (1978) and Waring et al. (1979), who produced negative pressure by using the method of equilibrium dehydration of wood samples over salt solutions, we used positive pressure from the pressure chamber. One cannot accurately estimate capillary water changes by using the pressure chamber because positive pressure cannot displace capillary water, or water that is held by surface tension at the air-water interface in either an embolized tracheid or between adjacent tracheids (Zimmermann 1983; Tyree and Yang 1990). The hypothesis of capillary water storage holds that water storage comes from the change in the radius of the meniscus between the cell wall and the gas space (Zimmermann 1983). If this hypothesis is correct, then maximum capillary water storage would be released at a pressure potential close to zero, and would stop before –0.6 MPa (Holbrook 1995; Tyree and Yang 1990). The high capacitance due to changes in the amount of capillary water represented half the water capacitance in *Thuja*, *Tsuga* and *Acer* but this capillary water storage has been interpreted to have no adaptive implication because it occurs when the environmental conditions are still favorable (Tyree and Yang 1990).

The only data of which we are aware for xylem capacitances using a similar method on saturated stem-woods are from Edwards and Jarvis (1982). Their values (estimated from Fig. 5) are very similar to the values we estimated for the first two phases of water change. They showed capacitances, which also corresponded to water release by cavitation events only, at –0.5 MPa ranging from 10% RWC MPa^{-1} for *Pinus contorta* D. to 20% RWC MPa^{-1} for *Picea sitchensis* B. and at 0.5–3.0 MPa ranging from 14% RWC MPa^{-1} for *Pinus contorta* D. to 22% RWC MPa^{-1} for *Picea sitchensis* B.

Trunk segmentation in relation to vulnerability to cavitation

As judged by the parameter Ψ_{50} (the water potential at which 50% of conductivity is lost), the overall outer sapwood is less vulnerable to cavitation than the overall inner sapwood. However, if we judge by Ψ_e (the air entry point), the overall inner sapwood is not significantly more vulnerable to cavitation than overall outer sapwood.

More intriguing is that at the base of the tree, Ψ_e and RWC do not differ significantly between inner and outer sapwood. The average inner sapwood values tend to be even more negative (Table 2). These results suggest that refilling of embolisms has been completed during the 29-year difference in wood age between these radial positions (Table 1). It would be interesting to test whether this pattern is conserved in a conifer with higher sapwood area such as *Pinus sylvestris* L., which can have up to 80 years worth of sapwood (Mencuccini et al. 1997), or *Pinus ponderosa* L., which can have up to 200 years (Ryan et al. 2000).

Although the resistance of water flow was higher in the top of the trunk (lower hydraulic specific conductivity), the tip of the trunk of Douglas-fir mature trees was less vulnerable to cavitation than the proximal (lower) parts. Wood higher up is modified (relative to basal wood) to be more resistant to cavitation than the wood at the base. Initial inspection of these data appears-inconsistent with the segmentation hypothesis (Tyree et al. 1983; Zimmerman 1983), which suggests that during severe drought, the loss of conductivity will develop primarily in the distal parts of the treeto protect the proximal part by stopping any water movement and thereby any water loss.

However, to assess the segmentation hypothesis relative to the tree's hydraulic architecture, one needs to know not only the parameters of the VCs throughout the trees, but also the most negative water potentials experienced. More research must be done to address this issue. The hydrostatic gradient causes water potentials to be lower at the top of the tree than at the base. However, the actual potential gradient will depend on the spatial and temporal patterns of conductivity, transpiration, and water storage. The lower Ψ_e at the top of the branched bole (node 35) parallels the hydrostatic gradient, suggesting that the air entry potential will be reached simultaneously in the base of the bole and in this intermediate position under static conditions of no transpiration. However, above node 35, the calculated water potential becomes more negative with height than one would predict based on the hydrostatic gradient alone (Fig. 6).

Relative hydraulic failure occurring in the trunk sapwood by position

Using the midday gradient of 0.019 MPa m^{-1} (Bauerle et al. 1999), a water potential of –1.5 MPa at the base of the tree and tree height of 43 m, we calculate that a difference of 0.8 MPa or 8% loss of hydraulic conductivity between the top and the bottom of the tree will be required to maintain the water column. This difference corresponds to a 13% loss of conductivity at the bottom, and a 5% loss in hydraulic conductivity at the top of the tree. Thus, there is a higher loss of conductivity at the bottom than the top of the tree. If we develop our scenario for a severe drought with a water potential of –2.5 MPa at the base of the tree, and use the same midday gradient, the difference in loss of hydraulic conductivity becomes even greater, with a 30% loss of conductivity at the bottom and a 15% loss of conductivity at the top of the tree.

For conifers, the drop in water potential is mainly confined to the branch ramifications (Tyree et al. 1983; Tyree 1988). In old-growth Douglas-fir (>450 years), the potential gradient is about 0.0105 MPa m^{-1} at predawn (statistically indistinguishable from the hydrostatic gradient, 0.0100 MPa.m^{-1}) and nearly twice as high at noon during a sunny day (Bauerle et al. 1999). Those reported midday gradients were for foliage high in the tree on

branches, not the leader, and the samples were not foil-covered, and therefore the 0.019 MPa m^{-1} used for our calculations overestimated the actual loss of conductivity that occurred in the trunk. The gross approximation made above for a loss of 5% in xylem hydraulic conductivity at the top of the tree follows Bond and Kavanagh's observations (1999) that leaf water potentials of upper branches of mature Douglas-fir typically generate less than 5% loss of xylem conductivity.

In the first study presenting the extent of xylem cavitation in mature Scots pine trees, Jackson et al. (1995) showed that the loss of conductivity at the base of the trunk (measured by acoustic emissions) occurred for water potentials as high as –1.2 MPa. Our study confirms that the lower parts of the trunk of mature Douglas-fir trees (from base to node 35) may operate close to the edge of hydraulic safety. However, the calculated values presented here on loss of hydraulic conductivity suggest that the main stem of the top (node 5) of the tree does not operate near a critical value for cavitation even when the bottom of the tree does so. This former result is in contrast with model predictions that distal parts of tree species operate near the edge of dysfunction for water transport (Tyree and Sperry 1988).

Ecophysiological implications: trade-off between water storage capacity and vulnerability to cavitation

For the young trees, the low capacitance found for the range of potentials over which the plants usually operate (between 0.5–3.0 MPa) suggests that their water uptake is linearly related to the water loss by the leaves. Few cavitation events occur at water potentials less negative than –3.8 MPa (Fig. 3a). Between the young trees and the mature trees, at a water potential more negative than the air entry point (–1.3 to –3.1 MPa, depending on height and radial position for the mature trees), the cells cavitated across the same range of xylem tension (the slopes s of the responses to an increase in water potential were around 30% loss of k_s MPa^{-1}, Fig. 3a, Table 3). This parameter s is species-dependent and may be related to the tracheids that have the largest pores in their pit membranes (Pammenter and Vander Willigen 1998).

In this paper we show that within the tree at high water potential ($>$–0.5 MPa), the base has a higher water storage capacity (water release by cavitation) than the top and is more vulnerable to cavitation than the top. Stored water is more accessible to the bottom part of the trees than the top and it can represent an important fraction of the water-use in dry conditions (Table 5). However, using –0.4 MPa as the maximum water potential encountered at the tree base (during the winter, from Domec and Gartner, unpublished data), we can estimate that RWC at the base of the trunk will never rise above 92%. In fact, 92% is an overestimate (caused by the methodological problem of measuring capillary water storage with a pressure bomb, as discussed above). This estimate contrasts with Waring and Running's report

(1978) that water content recovers fully in this species, but it is consistent with other studies that showed that, without generating positive pressure, xylem never fully rehydrates during the winter (Chalk and Bigg 1956; Jackson et al. 1995).

The similar values found for the biological range of water potential (between –0.5 and –3.0 MPa, Tables 5, 6) indicate that every location of the trunk behaves the same in terms of water storage whereas the tree top is much more resistant to cavitation. For the top of the trees, the trade-off associated with low vulnerability to cavitation is at a cost of low hydraulic conductivity and water storage capacity (Stratton et al. 2000). Increasing the vulnerability to cavitation by a factor of 2.0 is at the cost of decreasing the capacitance by a factor of 2.6 (data not shown) and the specific conductivity by a factor of 4.5 (Fig. 5a). The more resistant higher part of the trunk, without compromising its capacitance, could have two adaptive functions: protection of the main meristem against severe drought, and provision of water at the beginning of the growing season to support the growth of the leader before new xylem has been produced.

Limited data show that in going from juvenile (top of the tree) to mature wood (lower parts of the trunk) in Douglas-fir, there are changes by a factor of 1.7 in wood density, 4.5 in stiffness (Senft et al. 1985), and 2.9 in tracheid length (Megraw 1985). Our study shows that there is a change by a factor of 2.0 in the water potential at which embolism occurs. With higher C_{3-5} values, the mature wood is more efficient in using the water released by cavitation events for the more negative water potential near the edge of 50% loss of conductivity ($<$–3.0 MPa). Assuming that the stomata are closed at these water potentials, this feature may help the tree to survive until the next rain falls to mitigate cuticular water loss (Tyree et al. 1991).

In conclusion, we have proposed a simple technique for analysis of the VCs by determining coefficients that have a physiological significance and that can be compared easily among species, plant parts, and other studies. We also suggested a new technique for calculation of capacitances based on RWC adapted to the differences in the wood density of the samples. Our study shows that it is possible to study trunk water relations of mature trees and not solely branches by using the air injection method. Trunk xylem of Douglas-fir has a change of hydraulic properties from the inner to the outer sapwood as well as from the bottom to the top of the tree. We believe that thesefindings represent a new step in the understanding of tree-trunk water relations. We now have evidence that the main bole of mature Douglas-fir does play an adaptive role in preserving the whole tree from hydraulic failure. To better address the importance of the occurrence of cavitation and the seasonality of their repair, we are currently measuring the changes in trunk RWC and water potential by height and depth into sapwood in the field. These data will help us better to understand tree adaptation to its environment as well as the functional trade-offs between production of wood for water transport and its production

2214

for mechanical support. These current results will also be of interest to tree breeders, who are interested in minimizing the amount of juvenile wood in trees: our results suggest that this juvenile wood may be important for the tree during times of drought.

References

Alder NN, Pockman WT, Sperry JS, Nuismer S (1997) Use of centrifugal force in the study of xylem cavitation. J Exp Bot 48:665–674

Bauerle WL, Hinckley TM, Cermak J, Kucera J, Bible K (1999) The canopy water relations of old-growth Douglas-fir trees. Trees 13:211–217

Bond BJ, Kavanagh KL (1999) Stomatal behavior of four woody species in relation to leaf-specific hydraulic conductance and threshold water potential. Tree Physiol 19:503–510

Borghetti M, Edwards WRN, Grace J, Jarvis PJ, Raschi A (1991) The refilling of embolised xylem in *Pinus sylvestris* L. Plant Cell Environ 14:357–369

Chalk L, Bigg JM (1956) The distribution of moisture in the living stem in Sitka spruce and Douglas-fir. Forestry 29:5–21

Cochard H (1992) Vulnerability of several conifers to air embolism. Tree Physiol 11:73–83

Edwards WRN, Jarvis PG (1982) Relations between water content, potential and permeability in stems of conifers. Plant Cell Environ 5:271–277

Erickson HD (1960) The effects of storage conditions and time upon permeability of green sapwood. Proc Am Wood Preserv Assoc 56:156–165

Gartner BL (1995) Patterns of xylem variation within a tree and their hydraulic and mechanical consequences. In: Gartner BL (ed) Plant stems: physiology and functional morphology. Academic Press, San Diego, pp 125–149

Holbrook NM (1995) Stem water storage. In: Gartner BL (ed) Plant stems: physiology and functional morphology. Academic Press, San Diego, pp 105–124

Holbrook NM, Burns MJ, Field CB (1995) Negative xylem pressures in plants: a test of the balancing pressure technique. Science 270:1193–1194

Jackson GE, Irvine J, Grace G (1995) Xylem cavitation in two mature Scots pine forests growing in a wet and dry area of Britain. Plant Cell Environ 18:1411–1418

Kavanagh KL, Bond BJ, Gartner BL, Aitken SN, Knowe S (1999) Root and shoot vulnerability to cavitation in four populations of Douglas-fir seedlings. Tree Physiol 19:31–37

Lin RT, Lancaster EP, Krahmer RL (1973) Longitudinal water permeability of western Hemlock. I. Steady state permeability. Wood Fiber 4:279–289

Megraw RA (1985) Douglas-fir wood properties. Proceedings, Douglas-fir: Stand Management for the Future, June 18–20. University of Washington, Seattle, pp 81–96

Mencuccini M, Grace J, Fioravanti M (1997) Biomechanical and hydraulic determinants of tree structure in Scots pine: anatomical characteristics. Tree Physiol 17:105–113

Newman JA, Bergelson J, Grafen A (1997) Blocking factor and hypothesis test in ecology: is your statistics wrong? Ecology 78:1312–1320

Pammenter NW, Vander Willigen C (1998) A mathematical and statistical analysis of the curves illustrating vulnerability of xylem to cavitation. Tree Physiol 18:589–593

Panshin AJ, De Zeeuw C (1980) Textbook of wood technology, 4th edn. McGraw-Hill, New York

Running SW (1980) Relating plant capacitance to the water relations of *Pinus concorta*. For Ecol Manage 2:237–252

Ryan MG, Bond BJ, Law BE, Hubbard R, Woodruff D, Cienciala E, Kucera J (2000) Transpiration and whole-tree conductance in ponderosa pine trees of different heights. Oecologia 124:553–560

Salleo S, Hinckley TM, Kikuta SB, Lo Gullo MA, Weilgony P, Yoon TM, Richter H (1992) A method for inducing xylem emboli in situ: experiments with a field-grow tree. Plant Cell Environ 15:491–497

SAS (1996) SAS/STAT User's guide, release 6.12. SAS Institute, Cary, N.C., USA

Senft JF, Quanci MJ, Bendtsen BA (1985) Property profile of a 60-year-old Douglas-fir. Proceedings: juvenile wood: what does it mean to forest management and forest products? Forest Products Research Society, Portland, Ore., 17October 1985, pp 17–28

Siau JF (1984) Transport processes in wood. Springer, Berlin Heidelberg New York

Sparks JP, Black A (1999) Regulation of water loss in populations of *Populus trichocarpa*: the role of stomatal control in preventing xylem cavitation. Tree Physiol 19:453–459

Sperry JS (1995) Limitations of stem water transport and their consequences. In: Gartner BL (ed) Plant stems: physiology and functional morphology. Academic Press, San Diego, pp 95–104

Sperry JS, Ikeba T (1997) Xylem cavitation in roots and stems of Douglas-fir and white fir. Tree Physiol 17:275–280

Sperry JS, Saliendra NZ (1994) Intra- and inter- plant variation in xylem cavitation in *Betula occidentalis*. Plant Cell Environ 16:279–287

Sperry JS, Tyree MT (1988) Mechanism of water-stress-induced xylem embolism. Plant Physiol 88:581–587

Sperry JS, Donnelly RR, Tyree MT (1987) A method for measuring hydraulic conductivity and embolism in xylem. Plant Cell Environ 11:35–40

Spicer R, Gartner BL (1998a) Hydraulic properties of Douglas-fir (*Pseudotsuga menziesii*) branches and branch halves with reference to compression wood. Tree Physiol 18:777–784

Spicer R, Gartner BL (1998b) Hydraulic conductivity of compression wood in branches of Douglas-fir (*Pseudotsuga menziesii*). Plant Cell Environ 11:35–40

Stratton L, Goldstein G, Meinzer FC (2000) Stem water storage capacity and efficiency of water transport: their functional significance in a Hawaiian dry forest. Plant Cell Environ 23:99–106

Tyree MT (1988) A dynamic model for water flow in a single tree. Tree Physiol 4:195–217

Tyree MT, Sperry JS (1988) Do woody plants operate near the point of catastrophic xylem dysfunction caused by dynamic water stress: answer from a model. Plant Physiol 88:574–580

Tyree MT, Yang S (1990) Water storage capacity of *Thuja, Tsuga*, and *Acer* stems measured by dehydration isotherms. Planta 182:420–426

Tyree MT, Graham MED, Cooper KE, Bazos LJ (1983) The hydraulic architecture of *Thuja occidentalis*. Can J Bot 53:1078–1084

Tyree MT, Snyderman DA, Wilmot T, Machado JL (1991) Water relations and hydraulic architecture of a tropical tree (*Schefflera morotoni*). Plant Physiol 96:1105–1113

Tyree MT, Davis SD, Cochard H (1994) Biophysical perspectives of xylem evolution: is there a tradeoff of hydraulic efficiency for vulnerability to dysfunction? IAWA J 15:335–360

Waring RH, Running SW (1978) Sapwood storage: its contribution to transpiration and effect upon water conductance through the stems of old-growth Douglas-fir. Plant Cell Environ 1:131–140

Waring RH, Whitehead D, Jarvis PG (1979) The contribution of stored water to transpiration in Scots pine. Plant Cell Environ 2:309–317

Zimmermann MH (1983) Xylem structure and the ascent of sap. Springer, Berlin Heidelberg New York